View metadata, citation and similar papers at core.ac.uk
brought to you by CORE
provided by University of Hertfordshire Research Archive

Appl. Opt. **44**(27), pp.5754-5758 (2005)

Ice analog halos

Zbigniew Ulanowski

Science and Technology Research Institute, University of Hertfordshire, College Lane, Hatfield, Herts AL10 9AB, United Kingdom (z.ulanowski@herts.ac.uk)

Crystals of sodium fluorosilicate are used to produce easy to set up visual displays of atmospheric halos, including the 22° halo, the Parry and upper tangent arcs. Scattering phase functions for single ice-analog rosettes, including a rough one, and a column aggregate, measured in randomized orientation are also given. The phase functions show prominent halo features, with the exception of the rough crystal.

OCIS codes: 010.2940, 010.1310, 290.1090

1. Introduction

Cirrus clouds exert profound influence on the radiative balance of the atmosphere. However, present understanding of cirrus with respect to scattering properties is weak, which is mainly due to inadequate theoretical models and lack of knowledge concerning ice crystal size and shape. Consequently, cirrus clouds remain an area of significant uncertainty in current climate models. Since computation of scattering properties of ice crystals is difficult, both in situ and laboratory measurements are important.

A beautiful way in which cirrus clouds manifest themselves is through halos – faint circles, arcs and spots of white or colored light seen when sunlight or moonlight shines through thin ice-clouds. Cirrus is a nearly unique source of these displays because most of them are produced by the refraction of light passing through ice crystals. A whole variety of shapes can be observed, with names ranging from the prosaic to the evocative: 22° halo, circumzenithal arc, sundogs, sun-pillar and Parry arc.[1,2,3] Laboratory halo simulations have been attempted before. However, the materials used either did not have the correct, hexagonal shape, had wrong values of the refractive index[4] and/or resulted from refraction through single, macroscopic objects (prisms) which due to their size cannot represent atmospheric ice crystals for the purpose of studying light-scattering properties.[2,5-7]

An outstanding question concerning atmospheric halos is why they accompany cirrus clouds so rarely, at least at lower latitudes.[8] The presence of water droplets, liquid or frozen, is one possible explanation.[9] Small crystal size may also be responsible, because the halo peak is broadened as the size parameter is reduced. However, even quite small ice crystals – with hexagon diameters around 20 μm – can be expected to produce 46° and 22° halos.[8,10] While multiple scattering can in principle remove halos, they are also absent from thin cirrus. Departure from hexagonal symmetry or crystal complexity are also possible explanations. However, both geometric optics modelling and observations indicate that hollow crystals should produce halos.[11,12] Likewise, modelling of scattering from column aggregates shows pronounced halos.[13]

Roughness of crystal surfaces is a strong possibility, as it can lead to the removal of halo peaks from phase functions.[10,13] In reality, a combination of several mechanisms may be responsible for the scarcity of atmospheric halos.

Field measurements of scattering on ice in clouds are not only difficult but for correct interpretation they require the knowledge of the size and shape of observed crystals. This information is imprecise, especially for smaller sizes. Laboratory measurements on ice crystals are also very demanding as the particles have to be maintained in equilibrium with water vapor at low temperatures; moreover, control over ice crystal morphology is poor. These difficulties have recently been overcome by the development of realistic ice analogs.[14] The analogs are appropriate for use at optical wavelengths and include microcrystals suitable as a replacement for both simple and complex ice crystals. The material used to produce the analogs, sodium fluorosilicate Na_2SiF_6, has correct refractive index for ice at visible wavelengths (1.31) and leads to crystals of hexagonal symmetry. Apart from light scattering studies[14,15] the analogs have been used for the testing and calibration of several *in situ* ice probes, including the Small Ice Detector and the Cloud Particle Imager.[16] A tangible demonstration that the new ice analogs do indeed resemble real ice is provided by the halo displays described here.

2. The 22° halo

The ice analog crystals were grown on glass using a previously described procedure.[14] Briefly, 2 ml of saturated solution of sodium fluorosilicate was poured onto a 40 mm diameter watch-glass and allowed to evaporate to dryness at room temperature. While the procedure for producing the analogs is simple, caution is required because sodium fluorosilicate is classified as toxic, and can cause severe irritation of eyes and mucous membranes. Also, it must be noted that impurities present in the solution, including undissolved fluorosilicate, can affect crystal habit. The watch-glass containing dry crystals was illuminated with a beam of white light from a slide projector containing a metal plate with a 2 mm aperture in place of a slide. The light scattered by the crystals fell onto a paper screen with a circle of black card acting as a beamstop – see Fig. 1(a). The photographs shown here were taken in back projection; however, the displays are also clearly visible from the front of the screen. Either way, the result is a circle of bright spots with the inner radius corresponding to scattering angle of 22° – see Fig. 2(a). It is interesting to note slight coloration of the displays in Fig. 2: the inner edge of the circle is reddish while the outer one is tinged blue. This effect is due to dispersion – the refractive index of the analogs, like for ice, decreases with wavelength. As an alternative to a projector a laser can be used, but its beam should be expanded to include as much of the sample area as possible. If using a projector, an aperture placed between the projector and the sample will help to remove stray light.

The ice-analog sample used to produce the halo contained mainly hexagonal, column-shaped crystals – as can be seen on the Scanning Electron Microscope (SEM) image in Fig. 3, which shows the actual sample used to produce the displays in Fig. 2. Cirrus halos are the result of scattering on so many crystals that smooth displays are visible. In contrast, the analog halos are produced by only a few hundred crystals. As a result spots of light coming from individual crystals can clearly be seen, like in Fig. 2(a). However, by rotating the sample during exposure a smooth display can obtained, better resembling an atmospheric halo – Fig. 2(b).

3. The Parry arc

The Parry arc, which very rarely appears just above the 22° halo, has traditionally been thought to be produced by column-shaped ice crystals in a seldom-found orientation: not only aligned

horizontally, but with one pair of facets horizontal too – the crystals are "doubly oriented".[1,2] Alternatively, singly oriented thick plates may be responsible.[17] While there is no satisfactory aerodynamic explanation for either orientation, geometric optics simulations show that such orientations could in principle produce the Parry arc. To produce the image shown in Fig. 4(a) the sample of ice-analog columns used for the 22° halo display was tilted with respect to the incident light beam to simulate sunlight coming from an oblique direction – see the diagram in Fig. 1(b). Since the sample contained a large proportion of crystals with their prismatic facets parallel to the glass, as the SEM image in Fig. 3 shows, they had the required "Parry orientation". However, there were also many crystals which had only their long axes parallel to the glass surface (they were singly oriented) – these produced the so-called upper tangent arc, which is the lower of the two arcs in the image. For comparison, a simulation of this display computed using the HaloSim geometric optics program[18] is shown in Fig. 4(b). In the simulation, the Sun elevation is 20° and the crystals contain a mixture of 60% doubly-oriented (Parry) and 40% singly-oriented hexagonal prisms with ±2° angular dispersion. Video sequences showing the evolution of the Parry arc with changing solar elevation are available, together with many examples of ice analog images.[19]

4. The 9° halo

A common feature of the ice-analog halos is the presence of an inner circle corresponding to a scattering angle of about 10° – see Fig. 2. Rare low-angle halos, most notably at the scattering angle of 9°, are thought to be produced in the atmosphere by crystals with pyramidal ends,[1,2] possibly including bullet rosettes.[10] It would be tempting to speculate that the origins of the feature seen in this study and of the 9° atmospheric halo are the same. However, the ice-analog samples seldom contained crystals with pyramid-shaped ends. While crystals with hollow ends were sometimes present, more prevalent were crystals with a concave prismatic face – see Fig. 3. These crystals form on the surface of the growth solution, with the concave face pointing upwards, and they are the probable source of the 10° feature. It can be conjectured that such crystals are unlikely to be present in the atmosphere due to their asymmetry.

5. Halos from complex crystals

The ice-analogs were levitated in an electrodynamic trap so that their scattering properties could be measured.[14] Wide scattering angle range was obtained by combining a photodiode array between 0.5 and 5° with a fiber-optics array detection between 3 and 177°. Phase functions of single crystals in random orientation can be measured by subjecting the crystals to angular oscillations. The phase functions have been found to show more or less pronounced peak in the 22° region, even for complex crystals such as rosettes or aggregates.[15] Example phase functions are shown in Fig. 5. In all cases apart from the rough rosette the 22° halo peak is quite prominent.

Fig. 6 shows a simulation of a visual display resulting from single scattering due to the experimental phase function in Fig. 5 from the 93 μm aggregate (Rayleigh scattering is not included). An optical microscopy image of the aggregate is shown in Fig. 7. This crystal consisted of about 20 columns with hexagon diameters ranging from approximately 10 to 30 μm – corresponding to size parameters between about 60 and 170 at the wavelength of 550 nm. The 22° halo can be seen clearly, despite apparent complexity of the crystal that produced it.

6. Conclusions

Crystals of sodium fluorosilicate can be used to produce visual displays of atmospheric halos, including the 22° halo, the Parry and upper tangent arcs. The demonstrations are easy to set up, requiring not much more than a slide projector or a laser. The 22° halo feature can be seen clearly in phase functions for randomly-oriented, levitated analog crystals, including both rosettes and a column aggregate, but not for a rough rosette. This suggests that atmospheric halos should be visible even if highly complex crystals are present, as long as crystal surfaces are smooth.

This work was supported by the Natural Environment Research Council grant NER/T/S/2001/00203. The author wishes to acknowledge assistance from many colleagues, including Evelyn Hesse, Ian Tongue, Rajam Chandrasekhar, Bill Liley and Paul Kaye.

References

1. W. Tape, *Atmospheric Halos* (American Geophysical Union, Washington, 1994).
2. R. Greenler, *Rainbows, Halos, Glories* (Elton-Wolf Publishing, Milwaukee, 2000).
3. K. Sassen, J. Zhu, and S. Benson, "Midlatitude cirrus cloud climatology from the Facility for Atmospheric Remote Sensing. IV. Optical displays," Appl. Opt. **42**, 332-341 (2003).
4. J. O. Mattsson, L. Brring, and E. Almqvist, "Experimenting with Minnaert's Cigar," Appl. Opt. **39**, 3604-3611 (2000).
5. M. Vollmer, and R. Tammer, "Laboratory experiments in at-mospheric optics," Appl. Opt. **37**, 1557-1568 (1998).
6. M. Vollmer, and R. Greenler, "Halo and Mirage Demonstrations in Atmospheric Optics," Appl. Opt. **42**, 394-398 (2003).
7. B. Barkey, K. N. Liou, Y. Takano, W. Gellerman, and P. Sokolsky, "An analog light scattering experiment of hexagonal icelike particles. Part II," J. Atm. Sci. **56**, 613-625 (1999).
8. M. I. Mishchenko, and A. Macke, "How big should hexagonal ice crystals be to produce halos?," Appl. Opt. **38**, 1626-1629 (1999).
9. J. S. Rimmer, and C. P. R. Saunders, "Radiative scattering by artificially produced clouds of hexagonal plate ice crystals," Atm. Res. **45**, 153-164 (1997).
10. K. N. Liou, Y. Takano, and P. Yang, "Light scattering and radiative transfer in ice clouds," in: *Light Scattering by Nonspherical Particles: Theory, Measurements, and Applications*, M. I. Mishchenko, J. W. Hovenier, and L. D. Travis, eds., (Academic Press, San Diego, 2000), p. 431.
11. A. Macke, "Scattering of light by polyhedral ice crystals," Appl. Opt. **32**, 2780-2788 (1993).
12. K. Sassen, N.C. Knight, Y. Takano, and A. J. Heymsfield, "Effects of ice-crystal structure on halo formation: cirrus cloud experimental and ray-tracing modeling studies," Appl. Opt. **33**, 4590-4601 (1994).
13. P. Yang, and K. N. Liou, "Single-scattering properties of complex ice crystals in terrestrial atmosphere," Contr. Atmos. Phys. 7**1**, 223-248 (1998).
14. Z. Ulanowski, E. Hesse, P. H. Kaye, A. J. Baran, and R. Chandrasekhar, "Scattering of light from atmospheric ice analogues," J. Quantit. Spectr. Rad. Transf. **79-80C**, 1091-1102 (2003).
15. Z. Ulanowski, E. Hesse, P. H. Kaye, and A. J. Baran, "Light scattering by complex ice-analogue crystals," in *Proceedings 8th Int. Conf. Electromagnetic and Light Scattering by Nonspherical Particles*, F. Moreno, ed. (University of Granada, 2005), pp.297-300.

16. Z. Ulanowski, P. Connolly, M. Flynn, M. Gallagher, A. J. M. Clarke, and E. Hesse, "Using ice crystal analogues to validate cloud ice parameter retrievals from the CPI ice spectrometer data," in *Proceedings 14th Int. Conf. On Clouds and Precipit.*, G. A. Isaac, ed. (IAMAS, 2004) pp.1175-1178.
17. K. Sassen, and Y. Takano, "Parry arc: a polarization lidar, ray-tracing, and aircraft case study," Appl. Opt. **39**, 6738-6745 (2000).
18. L. Cowley, and M. Schroeder, HaloSim program, http://www.sundog.clara.co.uk/atoptics/phenom.htm.
19. Z. Ulanowski, "Ice-Analogue Halos," http://strc.herts.ac.uk/ls/halos.html.

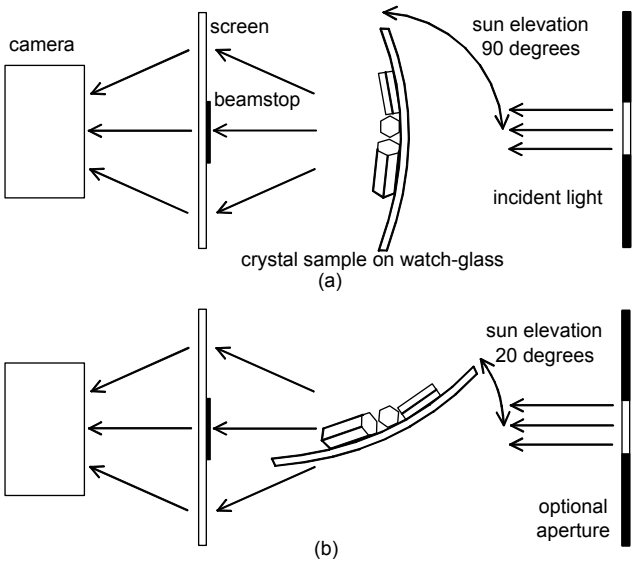

Fig. 1. Arrangement used to produce halos in the laboratory: in (a) the incident light is normal to the glass surface, in (b) the angle between the beam and the glass is about 20°.

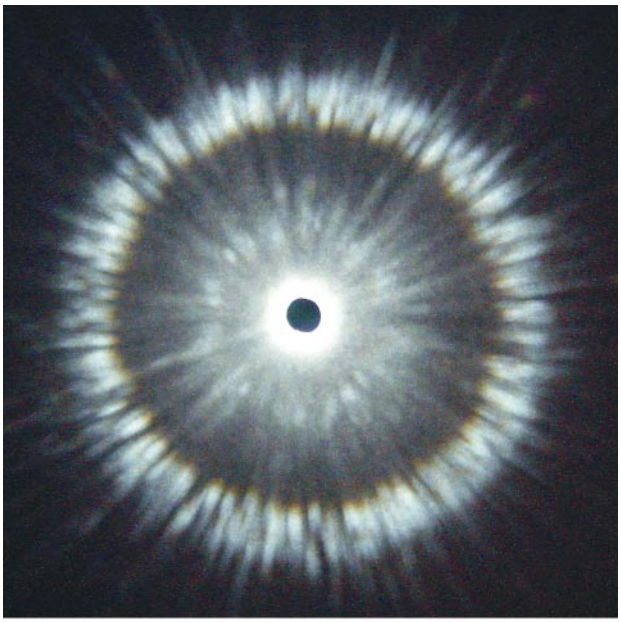

(a)

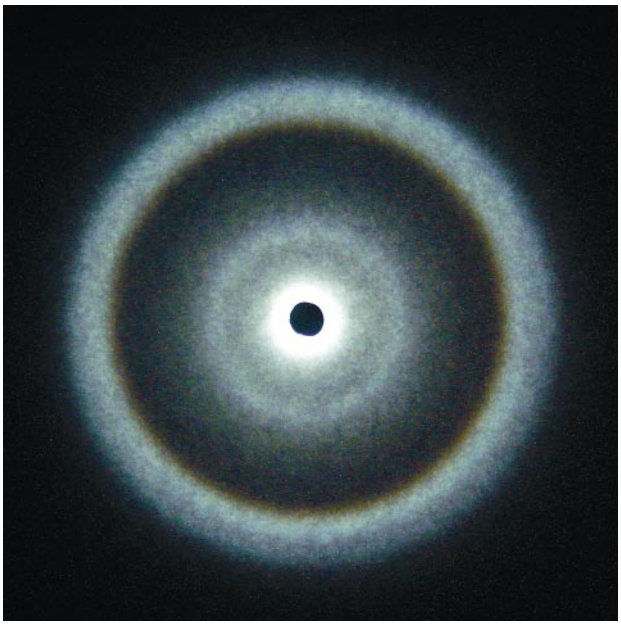

(b)

Fig. 2. Halo display produced by ice analog crystals on a watch-glass: (a) shows the 22° halo from a stationary sample, in (b) the sample was rotated during camera exposure.

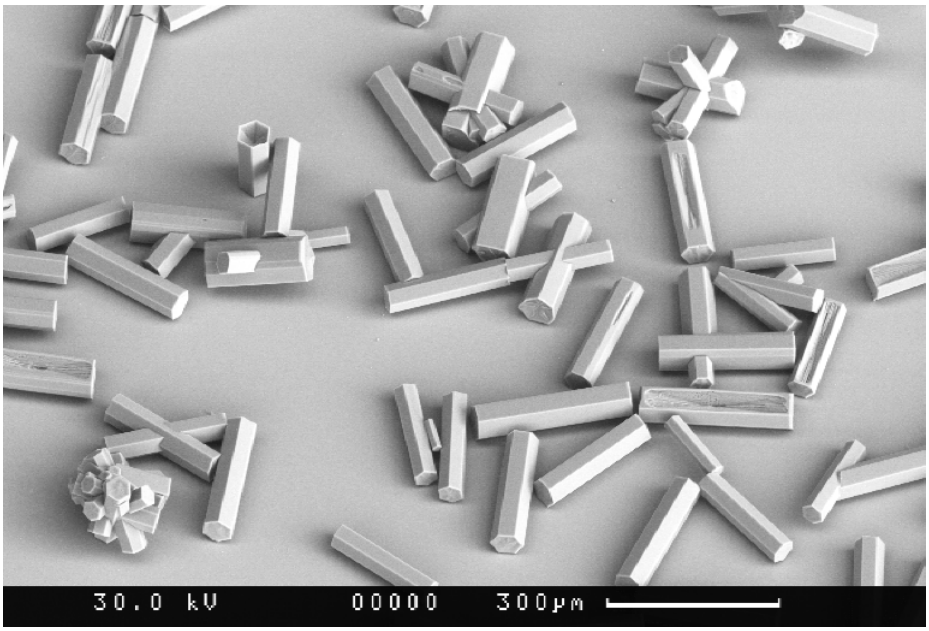

Fig. 3. SEM image of the ice analog sample used for producing the halo displays in Figs. 2 and 4.

(a) (b)

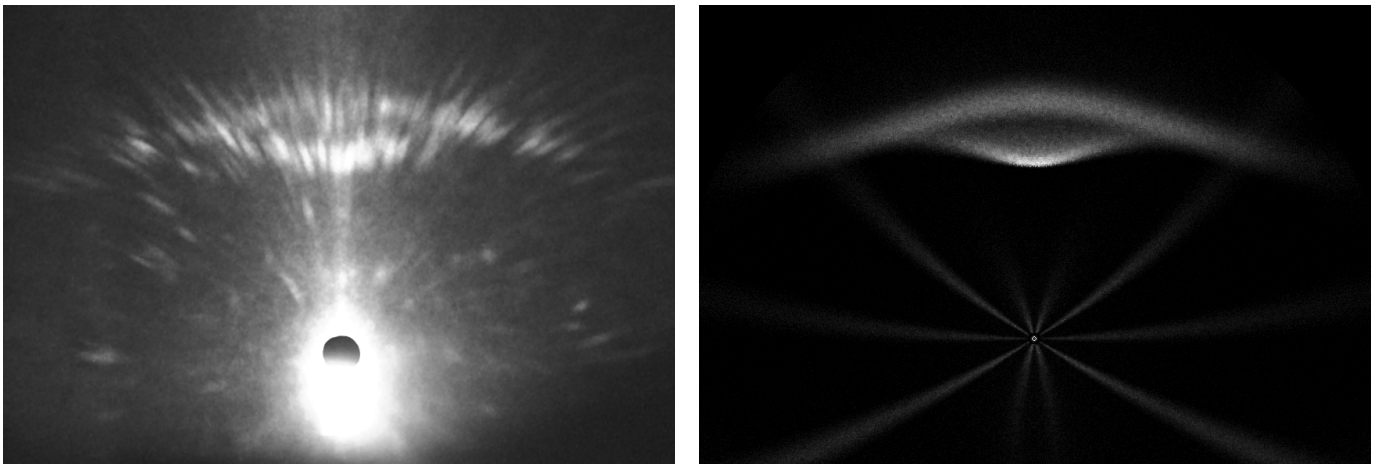

Fig. 4. Parry and upper tangent arc display: (a) produced by ice-analog crystals on a watch-glass tilted as in Fig. 1(b), and (b) modelled using the HaloSim geometric optics computer program.[18]

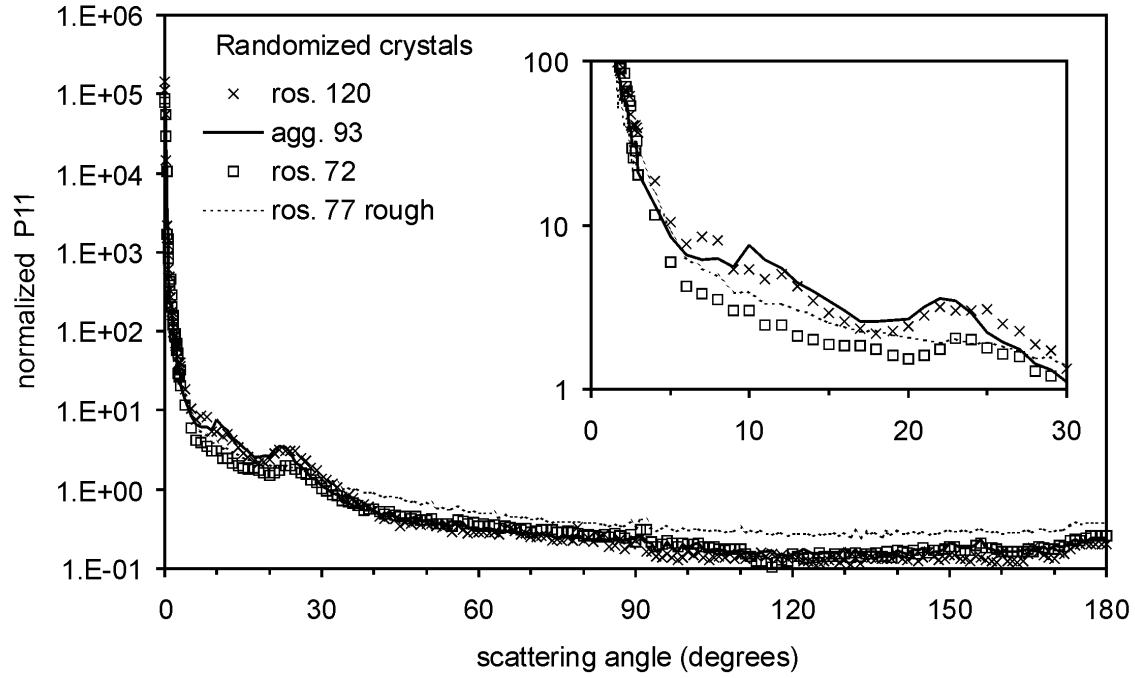

Fig. 5. Normalized phase functions measured for levitated, single ice-analog crystals. The inset shows the 0-30° region.

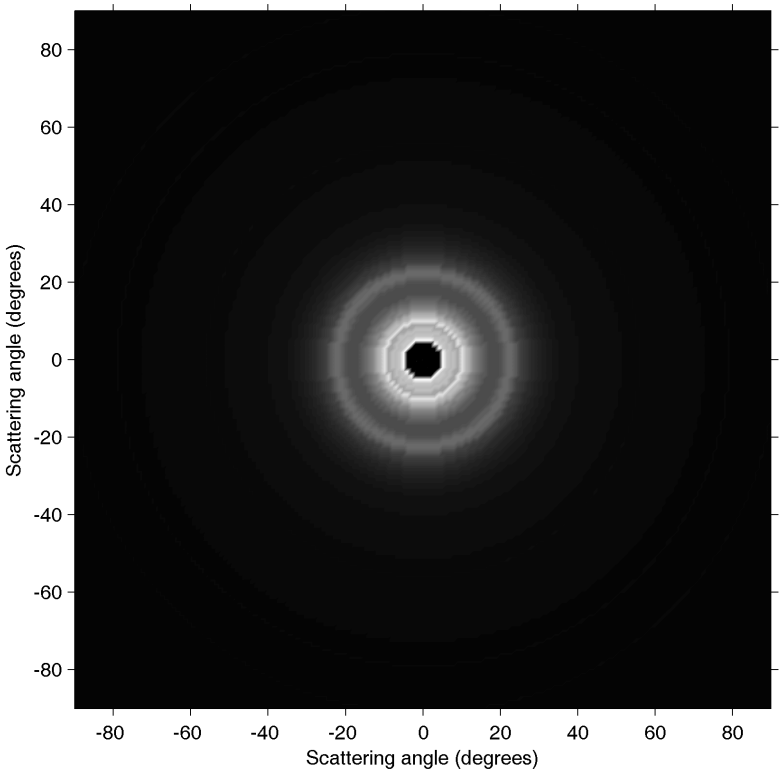

Fig. 6. Two-dimensional simulation of single scattering due to the phase function shown in Fig. 5. The source (Sun) is in the center.

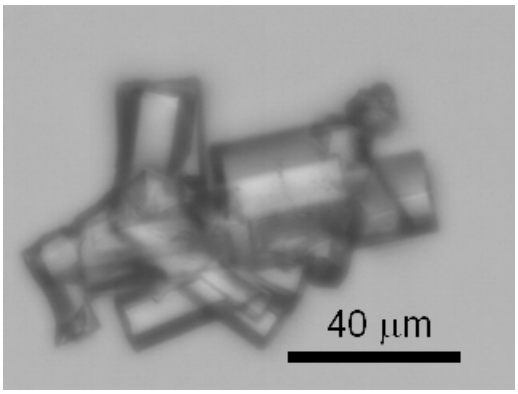

Fig. 7. Optical microscopy image of ice analog aggregate with a maximum dimension of 93 μm.